Reports

Label-free detection of surface markers on stem cells by oblique-incidence reflectivity difference microscopy

Kai-Yin Lo[1,3,*], Yung-Shin Sun[2,*], James P. Landry[2], Xiangdong Zhu[2], and Wenbin Deng[3]
[1]Department of Agricultural Chemistry, National Taiwan University, Taipei, Taiwan, [2]Department of Physics, University of California–Davis, Davis, CA, USA, and [3]Department of Cell Biology and Human Anatomy, Institute of Pediatric Regenerative Medicine, School of Medicine, University of California–Davis, Davis, CA, USA

BioTechniques 50:381-388 (June 2011) doi 10.2144/000113670
Keywords: Cell microarray; stem cell; label-free; oblique-incidence reflectivity difference (OI-RD)

*K.-Y.L. and Y.-S.S. contributed equally to this work.

Conventional fluorescence microscopy is routinely used to detect cell surface markers through fluorophore-conjugated antibodies. However, fluorophore-conjugation of antibodies alters binding properties such as strength and specificity of the antibody in often uncharacterized ways. Here we present a method using an oblique-incidence reflectivity difference (OI-RD) microscope for label-free, real-time detection of cell surface markers, and apply it to analysis of stage-specific embryonic antigen 1 (SSEA1) on stem cells. Mouse stem cells express SSEA1 on their surfaces, and the level of SSEA1 decreases when the cells start to differentiate. In this study, we immobilized mouse stem cells and non–stem cells (control) on a glass surface as a microarray and reacted the cell microarray with unlabeled SSEA1 antibodies. By monitoring the reaction with an OI-RD microscope in real time, we confirmed that the SSEA1 antibodies bind only to the surface of the stem cells and not to the surface of non–stem cells. From the binding curves, we determined the equilibrium dissociation constant (K_d) of the antibody with the SSEA1 markers on the stem cell surface. Thus, the OI-RD microscope can be used to detect binding affinities between cell surface markers and unlabeled antibodies bound to the cells; this information could be useful for determination of stem cell stages.

Pluripotent stem cells are capable of self-renewing and differentiating into various cell types in a living body. Embryonic stem (ES) cells are embryo-derived pluripotent cells that have so far served as the gold standard for research into the mechanisms of tissue formation and the development of disease, and provide a promising source of replacement cells for tissue repair. However, research with embryo-derived ES cells, particularly with respect to their use as disease models or transplantable replacement cells, has been hampered by regulatory hurdles impeding the derivation of new lines and by difficulties in obtaining patient-specific, histocompatible cells that would avoid immune rejection after transplantation. A recent breakthrough in stem cell research was reported by Yamanaka and colleagues who ectopically expressed four transcription factors—*Oct4*, *Sox2*, *Klf4*, and *Myc*—in murine and human fibroblasts and reprogrammed somatic cells into ES-like cells they have named induced pluripotent stem (iPS) cells (1–4). Because iPS cells can be derived from somatic cells, potential immune rejection and ethical considerations associated with the use of ES cells can be avoided by autologous transplantation (reviews in References 5–9).

Stem cell differentiation is a powerful tool for developmental biology and regenerative medicine (10–14). Differentiated rather than undifferentiated cells are better used as replacement cells for tissue repair to avoid tumorgenic potential. The state of stem cell differentiation can be distinguished by cell surface markers. At different developmental stages, cells present different markers on the surface. Mouse ES and iPS cells express a surface marker, stage-specific embryonic antigen-1 (SSEA1), on their surface, and its expression level decreases when the pluripotent cells become differentiated. In conventional immunocytochemical or flow cytometric methods, cell markers are detected by fluorescence-labeled antibodies. These methods detect the endpoint of the antibody-antigen reaction instead of its binding reaction kinetics (equilibrium dissociation constant K_d), which reveals both the presentation and population of the surface antigens from one developmental stage to another. Moreover, labeling antibodies with extrinsic fluorescent agents can alter strength and specificity of the antibody-antigen interactions (15,16). Quantitative RT-PCR is another method for detecting the expression level of cell surface markers, although the expression level of mRNA may not be directly correlated with that of proteins.

Here we present an oblique-incidence reflectivity difference (OI-RD) scanning microscope (17–21) as a label-free, real-time method for detection of cell surface antigen reaction with unlabeled antibodies. This method is capable of detecting interactions between solution-phase analytes and surface-immobilized

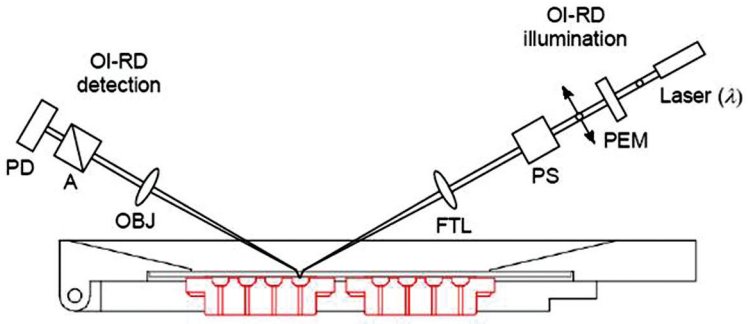

Figure 1. OI-RD schematic. Schematic of an OI-RD scanning optical microscope consisting of illumination and detection optics and a sample cartridge that holds a 1 in. × 3 in. functionalized glass slide and a fluidic inlet/outlet assembly for each of the eight chambers. By scanning a focused optical beam along the *y* axis (in and out of the plane) and moving the sample holding stage along the *x* axis (left to right), the scanner detects real-time changes in the microarray as a result of reaction or other processes by measuring the amplitude and phase changes of the reflected beam. PEM, photoelastic modulator; PS, phase shifter; FTL, *f*-theta lens; OBJ, objective; A, analyzer; PD, photodiode.

targets (DNA, proteins, or cells) in the microarray format. OI-RD signals are comparable to surface plasmon resonance (SPR) signals (usually expressed in resonant units, or RUs) (22) and can be converted into surface mass density (18). OI-RD microscopes have unique advantages over SPR-based instruments by allowing for simultaneous detection of more than 10,000 biomolecular interactions on a single slide (17) and working with chemically functionalized glass slides that are far more cost-effective. In this work, we demonstrated the effectiveness of the OI-RD microscope as a label-free optical sensor of the binding reaction kinetics of unlabeled antibodies to surface antigens on whole stem cells immobilized on aldehyde-functionalized glass slides.

Materials and methods

Cell culture conditions

We cultured mouse stem cells under two different conditions to obtain cells expressing different SSEA1 levels. Mouse embryonic stem (mES) cells (Invitrogen, Carlsbad, CA, USA) and mouse induced pluripotent stem (miPS) cells (RIKEN BioResource Center Cell Bank, Tsukuba, Ibaraki, Japan) were cultured in Dulbecco's modified Eagle's medium (DMEM; GIBCO, Invitrogen) supplemented with 20% defined fetal bovine serum (FBS; GIBCO), 2 mM L-glutamine, 1 mM sodium pyruvate, 0.1 mM β-mercaptoethanol, 1% nonessential amino acids (NEAA), and 1000 U/mL leukemia inhibitory factor (LIF) with feeder cells (AppliedStemCell, Menlo Park, CA, USA). Under the second condition, mES and miPS cells were cultured on gelatin-coded plates in the same medium without LIF. Under this condition, stem cells started to spontaneously differentiate in the absence of LIF and growth factors supplied from feeder cells. We labeled the cells as mES(D) and miPS(D) in the figures.

HEK293T cells and fibroblasts (A19; provided by Zhao-Qi Wang, Leibniz Institute for Age Research, Jena, Germany) were grown in DMEM supplemented with 10% FBS. Cells were grown at 37°C in a 5% CO_2 incubator to 70%–80% confluence. Cells were washed once with Dulbecco's phosphate-buffered saline (DPBS; GIBCO) and then treated with 0.05% trypsin for 2 min to make a single-cell suspension. Trypsin was neutralized with addition of FBS. Cells were collected in 15-mL tubes and spun down. Cells were pelleted and resuspended in 1-mL cold 1% paraformaldehyde in PBS for 15 min on ice. We washed cell pellets with DPBS twice to remove any residual medium and paraformaldehyde and resuspended in printing buffer (1× PBS with 20% Ficoll 400 plus 4% glycerol) at a cell density of approximately 10^7 cells/mL (23). Ficoll 400 was used to keep the cells resuspended in the solution, and glycerol was used to keep the cells hydrated.

Preparation of cell microarrays and procedures of subsequent reactions

We dispensed 50 μL cell suspension in a 384-well microplate and printed the solution on an aldehyde-coated glass slide (CEL Associates, Pearland, TX, USA) with an OmniGrid 100 contact-printing arrayer (Digilab, Holliston, MA, USA). Four replicates of each of the eight-cell suspensions, as well as a BSA solution, were also printed. Unmodified BSA spots at a concentration of 0.5 mg/mL in 1× PBS were printed as negative controls. After printing cells on

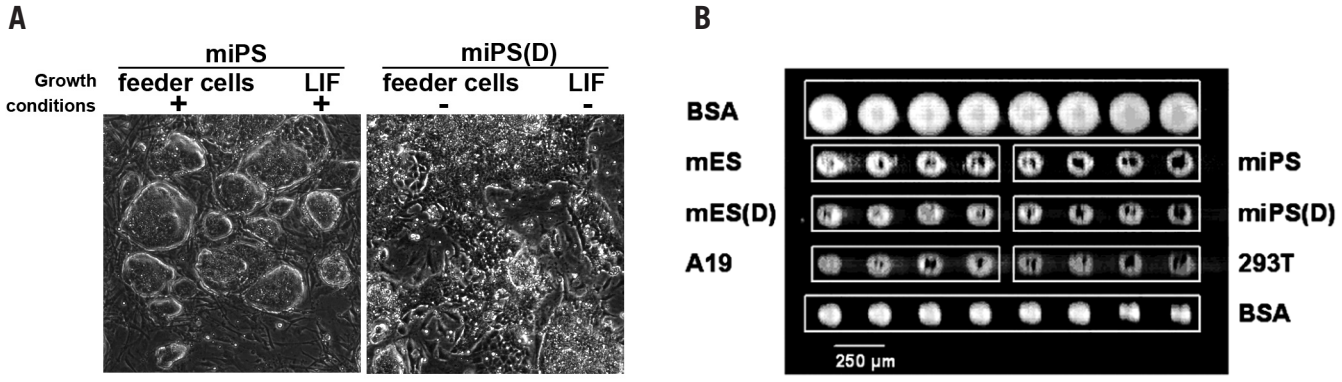

Figure 2. Morphology of stem cells and OI-RD image of printed cells on glass slides. (A) Stem cells were cultured on a six-well plate under two different culture conditions. Cell morphology was examined under a microscope with visible light (Nikon Diaphot 200). Left panel, stem cells were cocultured with feeder cells in the stem cell medium supplemented with LIF. Right panel, stem cells were grown in the mES medium without LIF and feeder cells. (B) Mouse stem cells at pluripotent or nonpluripotent stage [mES; mES(D); miPS; miPS(D)], fibroblast cells (A19), and HEK293T cells were trypsinized to single-cell suspension and resuspended in printing buffer (1× PBS with 20% Ficoll 400 plus 4% glycerol). Cells and BSA solution were spotted as a microarray onto the glass slide and detected with the OI-RD microscope.

aldehyde-coated slides, we stored these slides for ≥24 h in a humid chamber to make sure that cells were attached to the surface well. Afterward, the printed slide was assembled into the sample holder fitted for the OI-RD microscope. To block the remaining free aldehyde groups on the glass surface from nonspecific reaction with protein probes, we exposed the printed surface to a flowing BSA solution at 0.5 mg/mL in 1× PBS for 1 h and then washed the surface with a flow of 1× PBS for 30 min. For reaction, we replaced 1× PBS buffer in the sample cartridge assembly with a solution of anti-SSEA1 antibody (24) or anti-biotin antibody as negative control at a flow rate of 30 mL/min for 3 s and then slowed down the flow rate to 0.05 mL/min during the remainder of the reaction. To observe the dissociation of the captured protein probes, we replaced the protein solution with 1× PBS at a flow rate of 30 mL/min for 3 s and then slowed down the flow rate to 0.05 mL/min during observation.

OI-RD scanning microscope for label-free detection

The OI-RD scanning microscope used in the present work was described in an earlier publication (18). An OI-RD microscope with an eight-chamber sample cartridge is shown in Figure 1. With this eight-chamber design, over 300 molecular targets can be interrogated simultaneously against eight analytes on a single glass slide. A *p*-polarized He-Ne laser beam at $\lambda = 633$ nm passes through a photoelastic modulator (PEM) so that the output beam is polarization-modulated at $\Omega = 50$ kHz. The beam passes through a phase shifter (PS) that adds an adjustable phase between the *p*-polarized and *s*-polarized components of the beam. An *f*-theta lens (FTL) focuses the beam onto the microarray-covered glass surface. By scanning in both *x*- and *y*-directions, the reflected beam passes through an analyzer (A) before forming (with an objective lens) an image onto a photodiode (PD). This laser beam is reflected off a glass slide surface covered with a target microarray. When the surface is exposed to a probe solution, a layer of probe molecules is captured in the region where the "hit" targets are printed. As a result, the magnitude and phase of the electromagnetic field associated with the reflected light from these regions change, but by different amounts, depending on the polarization state of the incident light beam. The OI-RD scanning microscope directly measures the differential changes between the *p*-polarized component and the *s*-polarized component of the reflected light. Such a difference is proportional to the surface mass density change brought about by the captured probe molecules. Basically, we measure the complex differential reflectivity change ($\Delta_p - \Delta_s$) across a microarray-covered glass surface (25). The physical properties of a surface-bound molecular layer on a glass surface are related to $\Delta_p - \Delta_s$ by (18,20,21)

$$\Delta_p - \Delta_s \cong -i\left[\frac{4\pi\varepsilon_s^{1/2}\varepsilon_0\sin^2\varphi_{inc}\cos\varphi_{inc}(\varepsilon_d-\varepsilon_s)(\varepsilon_d-\varepsilon_0)}{(\varepsilon_0-\varepsilon_s)(\varepsilon_0\cos^2\varphi_{inc}-\varepsilon_s\sin^2\varphi_{inc})\varepsilon_d}\right]\times\left(\frac{\Gamma}{\lambda\rho}\right). \quad \text{[Eq. 1]}$$

φ_{inc} is the incidence angle of illumination; ε_0, ε_d, and ε_s are the respective optical constants of aqueous ambient, the molecular layer (e.g., printed cells or captured proteins), and the glass slide at $\lambda = 633$ nm. In our present study, $\varphi_{inc} = 36.63°$C, $\varepsilon_s = 2.307$ for glass slide, $\varepsilon_0 = 1.788$ for aqueous buffer, and $\varepsilon_d = 2.031$ for cells and proteins in solution. Γ is the surface mass density (in g/cm^2) of the molecular layer, and $\rho = 1.35$ g/cm^3 is the volume density of aqueous proteins. An image of a cell microarray was acquired with pixel dimensions of 20 µm × 20 µm. To acquire binding curves, we selected one target pixel in the middle of a printed spot and two reference pixels in the unprinted regions adjacent to the printed spot and measured the optical signals from these pixels repeatedly at a time interval that is short compared with the characteristic time of the reaction. We took the difference between the signal from a target pixel and the averaged signal from the two reference pixels as the final signal. This minimized the contribution of the drift in the optical system to the measurement.

Immunofluorescence and microscopy

After cells were printed as described above, the slide was blocked with blotting-grade 3% BSA (Promega, Madison, WI, USA) for 1 h at room temperature and then incubated with mouse anti-SSEA1 (24) in blocking buffer at 4°C overnight. After washing three times with PBS, cells were incubated with fluorescein isothiocyanate (FITC)-conjugated secondary antibody (Invitrogen) for 1 h at room temperature. Fluorescence was visualized on a microscope (Nikon Diaphot 200; Nikon, Melville, NY, USA) fitted with a digital camera. Images were prepared using Adobe Photoshop (Adobe Systems, San Jose, CA, USA).

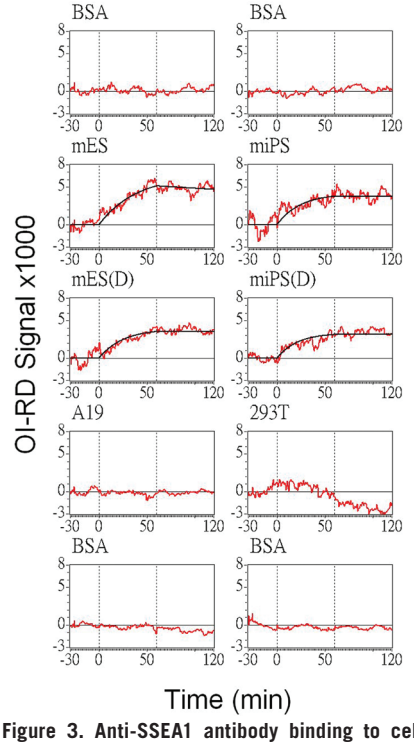

Figure 3. Anti-SSEA1 antibody binding to cell microarray. Real-time binding curves (in red) as measured with OI-RD microscopy of the anti-SSEA1 antibody at 10 nM reacting with surface-immobilized cells and BSA spots. The two vertical dashed lines are the start of the association and dissociation phases, respectively. Solid black lines are the fitted Langmuir curves, as shown for the different types of mouse stem cells. mES, mouse embryonic stem; miPS, mouse induced pluripotent stem; mES(D), differentiated mES cells; miPS(D), differentiated miPS cells; A19, fibroblasts; 293T, HEK293T cells.

Flow cytometry

Cells were trypsinized and stained with 1:50 anti-SSEA1 antibody followed by 1:1000 IgM goat-anti-mouse Alexa 488 conjugated antibody (Invitrogen). Flow cytometry and analysis were performed on a CyAn ADP instrument (Dako Cytomation, Dako, Carpinteria, CA, USA).

Results and discussion

Immobilization of stem cells and control cells on functionalized glass slides

To generate stem cells in different differentiation states, we cultured mES cells and miPS cells in a six-well plate under different conditions: (*i*) on a layer of feeder cells (mouse embryonic fibroblasts), which could provide growth factors necessary for maintenance of pluripotency (regular cultures, labeled as mES and miPS), and (*ii*) in the same medium but without coculturing with feeder cells nor the addition of any growth factors [differentiated (D) cultures, labeled as mES(D) and miPS(D)]. Cells were maintained at ~70% confluence. As shown in Figure 2A, after incubation for 2 weeks, stem cells were found to maintain colony shape and clear edge when grown with feeder cells (Figure 2A, left panel). When the stem cells were grown in the medium without any growth factors, either by secretion from feeder cells or addition of LIF, a common growth factor used in mouse stem cell cultures, cells lose colony shape and become flat (Figure 2A, right panel). This phenotype indicated that stem cells were losing their pluripotency. We also performed flow cytometry using anti-SSEA1 antibody to quantify the number of SSEA1 positive cells. Only 40% of mES(D) and miPS(D) cells, compared with 80% of mES and miPS cells, were SSEA1-positive (data not shown).

We used OI-RD to distinguish these stem cells at different differentiation states by using an anti-SSEA1 antibody to react with the surface antigen on pluripotent stem cells. We used A19 fibroblasts and HEK293T cells as controls, as they are not stem cells and do not express the SSEA1 surface antigen.

Figure 2B shows the OI-RD image of a printed cell microarray after washing with 1× PBS. The spot size is ~130 μm in diameter (except for the very top row of BSA, which has a diameter of about 200 μm), and the center-to-center spacing is approximately 250 μm. In the *x*-direction, the microarray contains four replicate spots of each of the six different types of cells in the middle three rows, together with eight replicate spots of BSA in the very top and bottom rows. The spots of cells (the middle three rows) are different from spots of BSA (the top and bottom rows), by having some dark regions in the spots. This is because cells are large and cause the incident light to scatter when it is reflected from the region where cells gather together. This observation is useful in determining whether cells are successfully immobilized on the glass surface.

We have tested different printing conditions for immobilizing cells on functionalized glass slides. Printing buffer was crucial to the morphology, density, and detected OI-RD signal of printed cell spots. Since OI-RD microscopes detect signals from all biomolecules within a printed spot, in order to avoid nonspecific signals from background proteins, the cell culture medium should be washed off and replaced with printing buffer. Also, cells resuspended in 1× PBS-only buffer tended to precipitate in the bottom of wells, which diminished the density of printed cells. Therefore, a printing buffer containing 1× PBS with 20% Ficoll 400 (Sigma-Aldrich, St. Louis, MO, USA) and 4% glycerol was used to keep cells suspended in the solution, as well as keep cell spots hydrated after printing. Glass slides coated with different chemical groups such as epoxy-lysine and poly-lysine were also tested for immobilization, but the morphology of spots was not ideal. Aldehyde-functionalized slides were used, because they gave better spot morphology and density (data not shown). In addition, a tested and selected cell density of 10^7 cells/mL was used for printing, to ensure that enough but not too many cells were immobilized on the surface. If the amount of printed cells is too low, the corresponding optical signals could be too weak. If the amount is too high, the binding affinity could be inaccurate, as mass transport effect would take place. In one spot, there are about 12–20 cells (as counted in immunofluorescent images). In the OI-RD image of the cell microarray, those dark regions in the middle of cell spots were the result of incident light scattering from where cells gather together densely.

Table 1. Binding rates (k_{on}, k_{off}, and K_d) between the anti-SSEA1 antibody and specific cells

	mES	mES(D)
k_{on} $(nM\ s)^{-1}$	4.01 ± 0.20 × 10^{-5}	6.76 ± 0.30 × 10^{-5}
k_{off} $(s)^{-1}$	2.65 ± 0.30 × 10^{-5}	0.58 ± 0.50 × 10^{-5}
K_d (nM)	0.670	0.090
	miPS	**miPS(D)**
k_{on} $(nM\ s)^{-1}$	7.05 ± 0.40 × 10^{-5}	7.96 ± 0.40 × 10^{-5}
k_{off} $(s)^{-1}$	0.71 ± 0.60 × 10^{-5}	0.60 ± 0.30 × 10^{-5}
K_d (nM)	0.110	0.077

Anti-SSEA1, anti-stage–specific embryonic antigen 1; mES, mouse embryonic stem; miPS, mouse induced pluripotent stem; mES(D), differentiated mES cells; miPS(D), differentiated miPS cells.

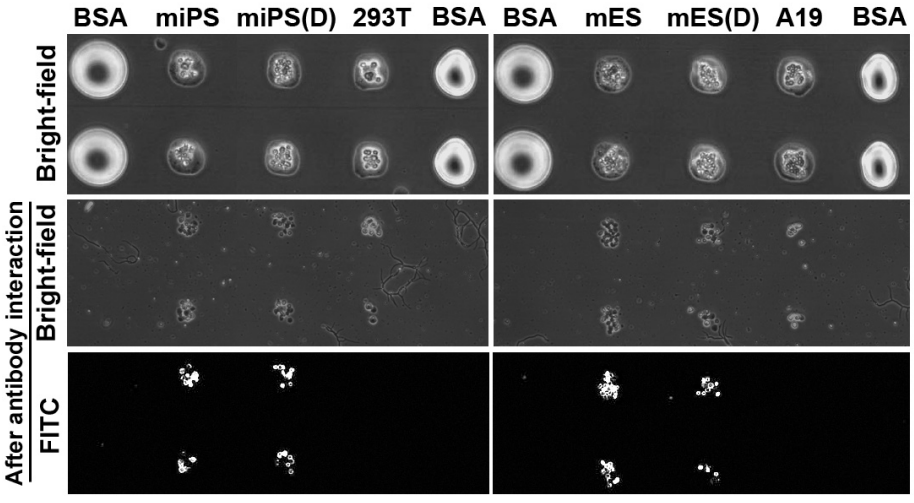

Figure 4. Immunofluorescence detection of cells with the stage-specific embryonic antigen 1 (SSEA1) marker. In the top panel, printed BSA spots and cells were visualized directly under a conventional (bright-field) microscope before washing. In the middle and bottom panels, the slide of printed cells was stained with a 1:1000 dilution of the anti-SSEA1 antibody and fluorescein isothiocyanate (FITC)–conjugated secondary antibody and examined by microscope under bright field (middle panel) and fluorescence (bottom panel) microscopy, respectively.

Interaction between stem cells and antibodies detected by the OI-RD microscope

After printing the cells on aldehyde-coated glass slides, we incubated the slides with a BSA solution to block remaining aldehyde groups, so that they later could not bind to antibodies nonspecifically in the subsequent reaction. Afterward, the microarray was reacted with the anti-SSEA1 antibody. Figure 3 shows the association-dissociation curves of anti-SSEA1 antibody at the concentration of 10 nM with the printed cell microarray. One unit of the optical OI-RD signal, 1×10^{-3}, corresponds to a surface mass density $\Gamma = 44$ ng/cm^2 of the captured aqueous proteins. The maximum OI-RD signal of 5×10^{-3} for mES at the end of the association phase corresponds to a layer of the captured anti-SSEA1 IgG with a density of 220 ng/cm^2, ~20% of a full monolayer of aqueous IgG molecules (18). For each cell or BSA spot, one representative curve was selected for display. The two vertical dashed lines correspond to the starts of association and dissociation, respectively. The results show that the anti-SSEA1 antibody binds to mES, miPS, mES(D), and miPS(D), but not A19, 293T, and BSA (Figure 3), indicating the specificity of interaction between the antibody and the surface antigens on the stem cells. The microarray was also reacted with antibiotin antibodies as control, and no positive signal was observed (data not shown).

As shown in Figure 3, the binding curves of the anti-SSEA1 antibodies in reaction with the immobilized cells and BSA were fitted to the one-to-one Langmuir reaction model (26). The fitting parameters k_{on}, k_{off}, and $K_d = k_{off}/k_{on}$ are listed in Table 1. The noise in the optical data was used to extract the error bars shown in the table. With k_{on} in the order of 10^{-5} (nM s)$^{-1}$ and k_{off} in the order of $10^{-6} \sim 10^{-5}$ (s)$^{-1}$, the equilibrium dissociation constant K_d for the cell-antibody interactions is in the ~10^{-2}–10^{-1}-nM range. Lower K_d values correspond to higher binding affinities. We find that mES and miPS have higher K_d than mES(D) and miPS(D). Thus, more differentiated cells show a lower K_d for the anti-SSEA1 antibody.

Considering that the number of the SSEA1 surface markers on pluripotent stem cells should be higher than on nonpluripotent stem cells, it may be somewhat surprising that anti-SSEA1 antibody shows higher binding affinity with the more differentiated cells. There are two possible reasons for this interesting observation. One is mass transport effect. The kinetics of the binding reaction can be significantly affected by the density of immobilized receptor targets, due to mass transport effect (27,28), if the mES cells express a near saturation level of SSEA1 surface markers, and it takes time for the antibodies to reach densely packed surface antigens with the proper orientation. Another more likely reason is the presentation of the SSEA1 surface markers at different stages of differentiation. Given that the surface markers may be at low densities on stem cells during differentiation, it is quite possible that the binding of the antibody might be more or less independent of the density, and we could attribute the variation in binding affinity constants (or equilibrium dissociation constants) to variation in the presentation of the surface markers. It is tempting to speculate that the binding affinity constants (or binding reaction kinetics) can be detected without fluorescence labeling as useful markers of stem cell differentiation instead of surface marker density. The biological significance of the binding affinity constants for monitoring stem cell differentiation remains to be further determined.

Confirmation of the SSEA1 surface antigen on immobilized stem cells with immunofluorescence microscope

To verify the results obtained by the OI-RD microscope, we monitored the change in SSEA1 surface antigens by conventional fluorescence microscopy. Right after printing, BSA spots and cells can be seen on the glass slide under the conventional (bright-field) microscope (Figure 4, top panels). The glass slide was incubated with the anti-SSEA1 antibody overnight, washed with PBS three times, and then incubated with FITC-conjugated secondary antibody. After washing, extraneous material (such as salt crystals from the printing buffer) were removed, and only the immobilized cells were visible under the conventional (bright field) microscope (Figure 4, middle panels). Under the fluorescent microscope, we observed that the anti-SSEA1 antibody indeed bound to pluripotent or differentiated stem cells, but not HEK293T cells or A19 fibroblast cells (Figure 4, bottom panels). These results confirm the findings with the OI-RD microscope. However, the OI-RD measurement provides additional information on the binding reaction kinetics that is lacking from fluorescence-based detection.

In conclusion, we show that the OI-RD microscopy method can be used to (*i*) detect the association between unlabeled antibody and a surface antigen; (*ii*) measure the binding affinities (e.g., equilibrium dissociation constant or K_d) between antibody and antigen; and (*iii*) detect hundreds of samples on a microarray platform. This report is the first study to directly measure the binding affinity between antibody and antigen on cell surface. In contrast to traditional cell surface studies, in which only the relative number of cell surface antigens can be determined, OI-RD microscope enables a dynamic characterization of surface antigens. With this powerful tool, we can detect the amount of and changes in affinity of cell surface markers as an independent monitor of developmental stages. Furthermore, this technique may be more generally used to detect the change

in cell surface markers on many other cell types for research and clinical applications.

Acknowledgments

We thank Zhao-Qi Wang (Leibniz Institute for Age Research) for the A19 fibroblasts and U-Ging Lo for reagent preparation. This work was supported by grants from the National Institutes of Health (NIH; grants nos. R01NS061983 and R01ES015988 to W.D., and R01-HG3827 to X.D.Z.), the National Multiple Sclerosis Society (to W.D.), and Shriners Hospitals for Children (to W.D.). This paper is subject to the NIH Public Access Policy.

Competing interests

The authors declare no competing interests.

References

1. **Okita, K., T. Ichisaka, and S. Yamanaka.** 2007. Generation of germline-competent induced pluripotent stem cells. Nature *448*:313-317.
2. **Takahashi, K., K. Okita, M. Nakagawa, and S. Yamanaka.** 2007. Induction of pluripotent stem cells from fibroblast cultures. Nat. Protoc. *2*:3081-3089.
3. **Takahashi, K., K. Tanabe, M. Ohnuki, M. Narita, T. Ichisaka, K. Tomoda, and S. Yamanaka.** 2007. Induction of pluripotent stem cells from adult human fibroblasts by defined factors. Cell *131*:861-872.
4. **Takahashi, K. and S. Yamanaka.** 2006. Induction of pluripotent stem cells from mouse embryonic and adult fibroblast cultures by defined factors. Cell *126*:663-676.
5. **Andersson, E.R. and U. Lendahl.** 2009. Regenerative medicine: a 2009 overview. J. Intern. Med. *266*:303-310.
6. **Kiskinis, E. and K. Eggan.** 2010. Progress toward the clinical application of patient-specific pluripotent stem cells. J. Clin. Invest. *120*:51-59.
7. **Lengner, C.J.** 2010. iPS cell technology in regenerative medicine. Ann. N.Y. Acad. Sci. *1192*:38-44.
8. **Deng, W.** 2010. Induced pluripotent stem cells: paths to new medicines. A catalyst for disease modelling, drug discovery and regenerative therapy. EMBO Rep. *11*:161-165.
9. **Selvaraj, V., J.M. Plane, A.J. Williams, and W. Deng.** 2010. Switching cell fate: the remarkable rise of induced pluripotent stem cells and lineage reprogramming technologies. Trends Biotechnol. *28*:214-223.
10. **Dushnik-Levinson, M. and N. Benvenisty.** 1995. Embryogenesis in vitro: study of differentiation of embryonic stem cells. Biol. Neonate *67*:77-83.
11. **Keller, G.M.** 1995. In vitro differentiation of embryonic stem cells. Curr. Opin. Cell Biol. *7*:862-869.
12. **Pedersen, R.A.** 1994. Studies of in vitro differentiation with embryonic stem cells. Reprod. Fertil. Dev. *6*:543-552.
13. **Richards, M., C.Y. Fong, and A. Bongso.** 2010. Comparative evaluation of different in vitro systems that stimulate germ cell differentiation in human embryonic stem cells. Fertil. Steril. *93*:986-994.
14. **Rooney, G.E., G.I. Nistor, F.B. Barry, and H.S. Keirstead.** 2010. In vitro differentiation potential of human embryonic versus adult stem cells. Regen. Med. *5*:365-379.
15. **Kodadek, T.** 2001. Protein microarrays: prospects and problems. Chem. Biol. *8*:105-115.
16. **MacBeath, G.** 2002. Protein microarrays and proteomics. Nat. Genet. *32(Suppl)*:526-532.
17. **Fei, Y., J.P. Landry, Y. Sun, X. Zhu, X. Wang, J. Luo, C.Y. Wu, and K.S. Lam.** 2010. Screening small-molecule compound microarrays for protein ligands without fluorescence labeling with a high-throughput scanning microscope. J. Biomed. Opt. *15*:016018.
18. **Landry, J.P., Y.S. Sun, X.W. Guo, and X.D. Zhu.** 2008. Protein reactions with surface-bound molecular targets detected by oblique-incidence reflectivity difference microscopes. Appl. Opt. *47*:3275-3288.
19. **Sun, Y.S., J.P. Landry, Y.Y. Fei, X.D. Zhu, J.T. Luo, X.B. Wang, and K.S. Lam.** 2008. Effect of fluorescently labeling protein probes on kinetics of protein-ligand reactions. Langmuir *24*:13399-13405.
20. **Zhu, X., J.P. Landry, Y.S. Sun, J.P. Gregg, K.S. Lam, and X. Guo.** 2007. Oblique-incidence reflectivity difference microscope for label-free high-throughput detection of biochemical reactions in a microarray format. Appl. Opt. *46*:1890-1895.
21. **Zhu, X.D.** 2004. Oblique-incidence optical reflectivity difference from a rough film of crystalline material. Phys. Rev. B *69*:1-5.
22. **Zhu, X.D.** 2006. Comparison of two optical techniques for label-free detection of biomolecular microarrays on solids. Opt. Commun. *259*:751-753.
23. **Thirumalapura, N.R., A. Ramachandran, R.J. Morton, and J.R. Malayer.** 2006. Bacterial cell microarrays for the detection and characterization of antibodies against surface antigens. J. Immunol. Methods *309*:48-54.
24. **Solter, D. and B.B. Knowles.** 1978. Monoclonal antibody defining a stage-specific mouse embryonic antigen (SSEA-1). Proc. Natl. Acad. Sci. USA *75*:5565-5569.
25. **Thomas, P., E. Nabighian, M.C. Bartelt, C.Y. Fong, and X.D. Zhu.** 2004. An oblique-incidence optical reflectivity difference and LEED study of rare-gas growth on a lattice-mismatched metal substrate. Appl. Phys. A Mater. Sci. Process *79*:131-137.
26. **Morton, T.A., D.G. Myszka, and I.M. Chaiken.** 1995. Interpreting complex binding kinetics from optical biosensors: a comparison of analysis by linearization, the integrated rate equation, and numerical integration. Anal. Biochem. *227*:176-185.
27. **Michel, W., T. Mai, T. Naiser, and A. Ott.** 2007. Optical study of DNA surface hybridization reveals DNA surface density as a key parameter for microarray hybridization kinetics. Biophys. J. *92*:999-1004.
28. **Peterson, A.W., L.K. Wolf, and R.M. Georgiadis.** 2002. Hybridization of mismatched or partially matched DNA at surfaces. J. Am. Chem. Soc. *124*:14601-14607.

Received 6 November 2011; accepted 1 April 2011.

Address correspondence to Wenbin Deng (stem cells), Department of Cell Biology and Human Anatomy, Institute of Pediatric Regenerative Medicine, School of Medicine, University of California–Davis, Davis, CA, 95616, USA. e-mail: wbdeng@ucdavis.edu; or Xiangdong Zhu (OI-RD microscope), Department of Physics, University of California–Davis, Davis, CA, 95616, USA. e-mail: zhu@physics.ucdavis.edu